



# HHS Public Access

Author manuscript

ACS Synth Biol. Author manuscript; available in PMC 2022 December 06.

Published in final edited form as:

ACS Synth Biol. 2019 July 19; 8(7): 1673–1678. doi:10.1021/acssynbio.8b00469.

## An engineered *B. subtilis* inducible promoter system with over 10,000-fold dynamic range

Sebastian M. Castillo-Hair<sup>1</sup>, Masaya Fujita<sup>2</sup>, Oleg A. Igoshin<sup>1,3,4</sup>, Jeffrey J. Tabor<sup>1,3,\*</sup>

<sup>1</sup>Department of Bioengineering, Rice University, 6100 Main St., Houston, TX 77005, USA.

<sup>2</sup>Department of Biology and Biochemistry, University of Houston, 4800 Calhoun Rd., Houston, TX 77004, USA.

<sup>3</sup>Department of Biosciences, Rice University, 6100 Main St., Houston, TX 77005, USA.

<sup>4</sup>Center for Theoretical Biophysics, Rice University, 6100 Main St., Houston, TX 77005, Texas, USA

### Abstract

*Bacillus subtilis* is the leading model Gram-positive bacterium, and a widely used chassis for industrial protein production. However, *B. subtilis* research is limited by a lack of inducible promoter systems with low leakiness and high dynamic range. Here, we engineer an inducible promoter system based on the T7 RNA Polymerase, the lactose repressor LacI, and a chimeric T7lac promoter P<sub>T7lac</sub> integrated as a single copy in the *B. subtilis* genome. In the absence of IPTG, LacI strongly represses T7RNAP and P<sub>T7lac</sub> and minimizes leakiness. Addition of IPTG de-represses P<sub>T7lac</sub> and simultaneously induces expression of T7RNAP, resulting in very high output expression. Using green fluorescent and  $\beta$ -galactosidase reporter proteins, we estimate that LacI-T7 can regulate expression with a dynamic range of over 10,000, by far the largest reported for an inducible *B. subtilis* promoter system. Furthermore, LacI-T7 responds to similar IPTG concentrations and with similar kinetics as the widely used P<sub>hy-spank</sub> IPTG-inducible system, which we show has a dynamic range of at most 300 in a similar genetic context. Due to its superior performance, our LacI-T7 system should have broad applications in fundamental *B. subtilis* biology studies and biotechnological applications.

### Graphical Abstract

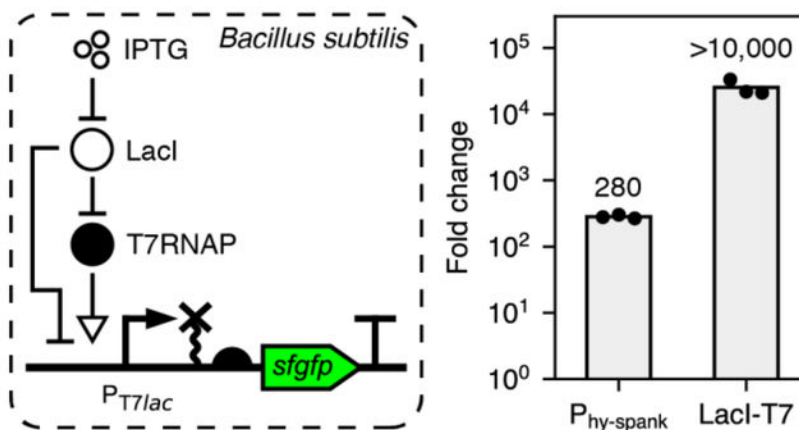
\*correspondence: jeff.tabor@rice.edu.

#### Author Contributions

S.M.C. and J.J.T. conceived of the project. S.M.C. designed and built DNA constructs, and performed flow cytometry, beta-galactosidase, and growth curve experiments. S.M.C. and M.F. performed western blot and immunoblotting experiments. S.M.C. performed all data analyses. O.A.I. and J.J.T. supervised the project. S.M.C., M.F., O.A.I., and J.J.T. wrote the manuscript.

#### Conflict of Interest Statement

A provisional patent on the *B. subtilis* LacI-T7 system is being filed by Rice University with J.J.T. and S.M.C. as inventors.



## Keywords

*Bacillus subtilis*; protein expression; inducible promoter system; IPTG; T7 RNA Polymerase

*Bacillus subtilis* is a model organism for studying Gram-positive bacterial biology and systems biology of cellular differentiation<sup>1</sup>, stress responses<sup>2</sup>, and multicellular organization<sup>3</sup>. Additionally, *B. subtilis* is among the most widely used hosts for protein production in the biotechnology industry due to its ability to secrete proteins into the cell medium, its non-pathogenic GRAS (generally recognized as safe) designation, and its high genetic tractability. For example, *B. subtilis* is used for large-scale production of lipases, proteases, and amylases, among other industrially-relevant proteins<sup>4,5</sup>.

Although many libraries of synthetic biological parts, such as constitutive promoters, RBSs, and degradation tags, have been reported for *B. subtilis*<sup>6-8</sup>, high-quality inducible expression systems with low leakiness and high expression are still needed. For example, biotechnology applications require inducible promoters capable of switching between a low production state for early-stage culturing and a high production state that maximizes protein yield during fermentation. Such parts are particularly important when the recombinant protein or metabolic pathway of interest are toxic to the host cells when overproduced<sup>9</sup>. Typical inducible promoters in *B. subtilis* have dynamic ranges (ratio of output protein expression in the presence versus absence of inducer) of at most a few hundred<sup>10-15</sup>. While a *B. subtilis* bacitracin-inducible promoter with a 1,000-fold range has been reported<sup>16</sup>, it requires antibiotic selection to maintain a multicopy plasmid, and its activity is transient and shuts down less than two hours after induction, likely due to an endogenous bacitracin stress response. In contrast, for the Gram-negative bacterium *Escherichia coli*, inducible promoters have been engineered with dynamic ranges greater than 1,000<sup>17-19</sup> or even 10,000<sup>20</sup>. Thus, improved *B. subtilis* inducible promoter systems are needed.

To address this issue, we engineered a stringent (i.e. non-leaky) and highly-inducible LacI-T7 promoter system for *B. subtilis*. Our system utilizes the hybrid  $P_{T7lac}$  promoter<sup>17</sup> to express a gene of interest, and the IPTG-inducible promoter  $P_{hy-spank}$ <sup>21</sup> to express the T7 RNA Polymerase (T7 RNAP) (Figure 1A). In the absence of inducer, LacI, which is constitutively expressed from the  $P_{penP}$  promoter<sup>10</sup>, represses both expression of T7



$\pm 0.033$  for  $P_{\text{hy-spank}}$ ), indicating that protein expression is more sensitive to changes in IPTG levels in the responsive range of the system. Finally, we characterized the response dynamics of both systems after an instantaneous addition of saturating IPTG (Figure 1F). As expected, both responses show an exponential-like increase until saturation. However, LacI-T7 responds slightly slower ( $t_{1/2} = 82.1 \pm 6.5$  min for LacI-T7,  $62.1 \pm 1.1$  min for  $P_{\text{hy-spank}}$ ), consistent with the need to produce an intermediate protein (T7RNAP) before expression of the reporter gene. In conclusion, LacI-T7 exhibits lower leakiness, higher maximal expression output, similar sensitivity to inducer, and much higher dynamic range than the widely used  $P_{\text{hy-spank}}$  system, albeit with a slightly slower response time.

The superior performance of LacI-T7 appears to arise from its unique design features. First, high maximal expression results from the use of T7 RNAP, a strong viral RNA polymerase which is capable of re-directing all bacterial resources towards expression of a single output gene<sup>27</sup>. In contrast, previous expression systems based on endogenous promoters are limited by the native transcriptional machinery and are subject to competition with other endogenous promoters. Second, leaky expression in the absence of inducer is reduced via the dual repression activity of LacI. In *E. coli*, a similar design has been shown to reduce basal expression by more than an order of magnitude compared to an unmodified  $P_{T7}$  output promoter<sup>17</sup>.

LacI-T7 should be useful in quantitative studies of *B. subtilis* biology. In particular, its stable single-copy chromosomal location and its low leakiness are desirable for analyses of ultrasensitive or excitable networks where low amounts of excess protein can cause cells to undergo dramatically different differentiation programs<sup>28</sup>.

We also expect LacI-T7 to be useful for heterologous protein expression applications. High expression from  $P_{T7lac}$  should enable high yields of both cytoplasmic and secreted proteins. Additionally, low leakiness in the absence of inducer should allow for fast initial cell growth, even with potentially toxic proteins. Furthermore, LacI-T7 is integrated into the *B. subtilis* genome, and thus will not suffer from plasmid instability issues<sup>29</sup> or require strong selective pressure to be maintained. Because it relies on the orthogonal T7 polymerase, LacI-T7 could also be ported to other industrially-relevant *Bacillus* species or strains with little additional work.

In conclusion, we have engineered a *B. subtilis* inducible promoter system with superior performance to current alternatives. Our system addresses important needs in fundamental and applied *B. subtilis* research.

## Methods

### DNA and strain construction

All cloning and experiments were performed in *B. subtilis* strain PY79<sup>30</sup>. Primers were ordered from Integrated DNA Technologies, Inc.  $P_{\text{hy-spank}}$  was amplified from integration plasmid pDR111<sup>21</sup>.  $P_{T7lac}$  was constructed via oligo annealing and extension. Synthetic RBS MF001 was obtained from integration plasmid pMF35<sup>31</sup>. Genomic homology fragments required for chromosomal integration were amplified from the purified genome

of *B. subtilis* PY79. A list of genetic parts, along with their sequences, can be found in Supplementary Table S1.

All systems were built as linear double-stranded integration module (IM), as we have previously described<sup>32</sup>. IMs contain the DNA of interest and a selection marker flanked by 1.5kb-long sequences homologous to the *amyE* locus of the *B. subtilis* genome where chromosomal integration via double crossover occurs. IMs were assembled from PCR-amplified parts using Golden Gate<sup>33</sup>. The resulting Golden Gate product was amplified using NEB Phusion DNA Polymerase and gel purified to obtain the IM. 500 ng was transformed into competent *B. subtilis* using standard transformation methods. The transformants were plated on selective media. Colonies were picked the next day and grown in LB media at 37 °C and 250 RPM for a few hours. Finally, freezer stocks were prepared with 700  $\mu$ L culture and 300  $\mu$ L 60% glycerol, and stored at -80 °C. This method avoids sub-cloning of integration plasmids in *E. coli*, as long as enough PCR-amplified DNA can be obtained. The complete sequences of all IMs constructed in this study can be found in Genbank via the following accession numbers: P<sub>hy-spank</sub>-*sfgfp*: [MN005205](#), LacI-T7-*sfgfp*: [MN005204](#), LacI-T7-*lacZ*: [MN005206](#).

For DNA sequence verification, an overnight LB culture was grown from a freezer stock, and 2  $\mu$ L saturated culture was used as template for a 50  $\mu$ L PCR reaction, either with Taq or Phusion DNA Polymerase. PCR products obtained in this fashion were gel-purified and sent for sequence verification to Genewiz, Inc.

### Codon optimization of *sfgfp*

Codon optimization of the N-terminal sequence of the *sfgfp* ORF was performed to decrease secondary structure with the RBS and increase translation efficiency. To do so, for each of the first 15 codons of the original *sfgfp* sequence<sup>22</sup>, a synonymous codon was chosen to reduce GC and increase AU content, with A preferred over U, with no regard for codon frequency. These changes were confirmed to increase the mRNA secondary structure free energy (and thus decrease secondary structure stability) via Nupack<sup>34</sup>, by using the sequence from the transcription start site up to the 90<sup>th</sup> nucleotide residue of the ORF. The complete optimized *sfgfp*\* sequence can be found in Supplementary Table S1.

### Media and Experimental Protocols

We used a modified M9 medium for all experiments. 1L 5xM9 salts at pH ~ 6.8 were prepared with 64 g Na<sub>2</sub>HPO<sub>4</sub>·7H<sub>2</sub>O, 15 g KH<sub>2</sub>PO<sub>4</sub>, 2.5 g NaCl, 5 g NH<sub>4</sub>Cl, 9.2 mL 6M HCl, and up to 1 L dH<sub>2</sub>O. For 1 L M9, we used 200 mL 5x M9 salts, 20 mL 10% casamino acids, 6.67 mL 60% glycerol, 1 mL 50 mM FeCl<sub>3</sub>/100 mM C<sub>6</sub>H<sub>8</sub>O<sub>7</sub> solution, 2 mL 50 mM MnSO<sub>4</sub>, 2 mL 1M MgSO<sub>4</sub>, 100  $\mu$ L 1M CaCl<sub>2</sub>, and dH<sub>2</sub>O up to 1 L.

For experiments in Figure 1B–D, an overnight LB culture was started from the freezer stock of each relevant strain. The next day, saturated cultures (OD<sub>600</sub> ~ 3) were diluted 10<sup>5</sup>-fold in M9. Media was distributed in culture tubes (3 mL per tube), inoculated with the appropriate inducers (0  $\mu$ M or 500  $\mu$ M IPTG), and incubated in a shaker operating at 250 rpm and 37 °C, until the OD<sub>600</sub> reached between 0.08 and 0.15 (around 6 hours). Culture tubes were then

transferred to an ice-water bath. 100  $\mu$ L of each sample was transferred to a flow cytometry tube containing 1 mL PBS for measurement.

For the experiment in Supplementary Figure 1, saturated overnight cultures of the two LacI-T7 strains were diluted  $10^5$ -fold in M9 media and distributed in two containers with 19 mL media each. IPTG was added to 500  $\mu$ M for only one container per strain. Media from each container was then distributed into six culture tubes (3 mL per tube) and incubated at 250 rpm and 37  $^{\circ}$ C. At the indicated timepoints, one tube per strain and IPTG condition was removed from the shaker, its OD<sub>600</sub> was measured using a spectrophotometer (Varian Cary 50 Bio), and the tube was discarded.

For the experiment in Supplementary Figure 2, saturated overnight cultures of each relevant strain were diluted  $10^5$ -fold in 50 mL M9 media, distributed in two 250 mL flasks each, and incubated in a shaker until an OD<sub>600</sub> of around 0.3. Then, IPTG was added to 1 mM for only one flask of each strain, and incubation continued for three additional hours. Whole cell lysates of each culture were prepared by sonication. Total proteins were fractionated by SDS-polyacrylamide gel electrophoresis (SDS-PAGE, 18%, 30:0.15 acrylamide:bis ratio) and detected by Coomassie brilliant blue staining. Immunodetection was carried out using polyclonal antibodies against GFP<sup>35</sup> and  $\sigma^A$ <sup>36</sup>. Primary antibodies were detected using an alkaline phosphatase coupled secondary antibody (Anti-rabbit IgG, Promega). A colorimetric detection system using nitro blue tetrazolium-5-bromo-4-chloro-3-indoyl phosphate (NBT/BCIP, Promega) as a substrate was utilized to detect the proteins of interest.

For experiments in Supplementary Figure 3, saturated overnight cultures of each relevant strain were diluted  $10^5$ -fold in M9 media, distributed in culture tubes, inoculated with inducers, and incubated in a shaker until an appropriate OD<sub>600</sub>, as described above.  $\beta$ -galactosidase assays were performed on each sample as previously described<sup>37</sup>. The reported  $\beta$ -galactosidase activity values were obtained by subtracting the measured activity of a wild-type PY79 negative control sample measured the same day from the measured activity of each sample.

For experiments in Figure 1E, saturated overnight cultures of each relevant strain were diluted  $10^5$ -fold in M9 media as above. Next, media was distributed across wells of a flat-bottom 24-well plate (Fisher 07-200-84), IPTG was added, and plates were sealed with adhesive foil (VWR 60941-126). Incubation and flow cytometry measurements were conducted as above.

For experiments in Figure 1F, saturated overnight cultures of each relevant strain were diluted  $10^5$ -fold in 25 mL M9 media contained in a 250 mL Erlenmeyer glass flask. Flasks were incubated as described above for 5:30h, after which IPTG was added to 500  $\mu$ M. Samples of 100  $\mu$ L were removed from each flask every 15 minutes and placed in flow cytometry tubes with 1mL PBS located in an ice-water bath. Flow cytometry measurements were conducted at the end of sample acquisition, as described above.

## Flow Cytometry Analysis

The sfGFP fluorescence distribution of each culture was measured using a BD FACScan flow cytometer with an excitation source of 488 nm and an emission window of 510/21 nm. 10,000 events were collected per sample. A suspension of calibration beads (Spherotech RCP-30–5A) in PBS was measured with each experiment. After data acquisition, raw .fcs flow cytometry files were processed using FlowCal<sup>24</sup>. Cell populations were gated by forward scatter/side scatter density (Supplementary Figure 4) retaining 50% of the total number of events. Next, fluorescence of each gated event in arbitrary units was converted into standardized MEFL values using the calibration bead data. The total cellular fluorescence of each culture sample was then obtained by calculating the median MEFL fluorescence of all gated events in that sample. Finally, the reported sfGFP fluorescence values were obtained by subtracting the total cellular fluorescence of a wild-type PY79 sample measured the same day from each sample's total cellular fluorescence. Numerical sfGFP fluorescence values of every sample and replicate can be found in Supplementary Data 1.

## Statistical analysis

Each experiment was replicated three times over different days. Fluorescence of each sample is reported as the mean  $\pm$  standard deviation of the sfGFP fluorescence from three experiments. A one-sample Student's t-test was conducted for every sample to evaluate whether sfGFP fluorescence was significantly different from zero (one-sided,  $p < 0.05$ ). Fluorescence of samples that failed this test are reported as "Not Detected" or "N.D."

## Growth model fitting

OD<sub>600</sub> data in Supplementary Figure 1 was fitted to an exponential growth model of the form:

$$x(t) = x_0 \cdot 2^{\frac{t}{t_d}}$$

Where  $x(t)$  is the OD<sub>600</sub> of the culture at time  $t$ ,  $x_0$  is the initial OD<sub>600</sub>, and  $t_d$  is the doubling time. Fitting was performed using the LmFit python package<sup>38</sup> with the Levenberg-Marquardt algorithm. To adequately fit low and high OD<sub>600</sub> values, the error to minimize was defined as the difference between the logarithm of an OD<sub>600</sub> datapoint and the logarithm of the model prediction.

## Transfer function fitting

Steady state transfer functions in Figure 1E were fitted to a Hill Function of the form:

$$y = y_0 + \Delta y \cdot \frac{x^n}{x^n + K_{1/2}^n}$$

Here,  $y$  is the observed sfGFP fluorescence in MEFL, which has a minimum value of  $y_0$  in the absence of inducer and a maximum of  $y_0 + \Delta y$  under saturating conditions,  $x$  is

IPTG concentration in  $\mu\text{M}$ ,  $K_{1/2}$  is the inducer concentration for half-maximum activation, and  $n$  is the Hill coefficient. Fitting was performed using the LmFit as described above. Experimental data from three replicates were combined and fitted simultaneously. Fitted parameter values and their uncertainties can be found in Supplementary Table S2 ( $P_{\text{hy-spank-sfgfp}}$ ) and Supplementary Table S3 (LacI-T7-*sfgfp*).

### Kinetic model fitting

The response of the  $P_{\text{hy-spank}}$  system to a step inducer addition was modeled as a differential equation system of the form:

$$\frac{dp}{dt} = k_p \cdot (c - p(t))$$

$$\frac{dg}{dt} = k_g \cdot (p(t) - g(t))$$

$$\frac{dG}{dt} = k_d \cdot (g(t) - G(t))$$

Here,  $p(t)$  represents the sfGFP production rate,  $g(t)$  represents immature sfGFP, and  $G(t)$  is the fully mature, observed sfGFP. Their dynamics are determined by rate constants  $k_p$ ,  $k_g$ , and  $k_d$ , the last of which corresponds to the cell growth rate. Finally,  $c$  is the system input. Units for  $c$ ,  $p(t)$ , and  $G(t)$  have been chosen such that, in steady state,  $c = p_{ss} = g_{ss} = G_{ss}$ , and thus  $c$  determines the steady state output fluorescence.

Similarly, the response of the LacI-T7 system to a step inducer addition was modeled as a differential equation system of the form:

$$\frac{dp}{dt} = k_p \cdot (c - p(t))$$

$$\frac{dr}{dt} = k_d \cdot (p(t) - r(t))$$

$$\frac{dg}{dt} = k_g \cdot (r(t) - g(t))$$

$$\frac{dG}{dt} = k_d \cdot (g(t) - G(t))$$

Where the additional term  $r(t)$  represents the T7 RNAP, whose dynamics are determined by  $k_d$  (cell division) just as with  $G(t)$ . Fitting was performed using LmFit as described above.



## Supplementary Material

Refer to Web version on PubMed Central for supplementary material.

## Acknowledgements

This work was supported by a Michel Systems Biology Innovation Award from Rice University and the National Institutes of Health (1R21AI115014-01A1). O.A.I. also acknowledges support from the National Science Foundation (MCB-1616755) and the Welch Foundation (Grant C-1995).

## References

- Narula J et al. Chromosomal Arrangement of Phosphorelay Genes Couples Sporulation and DNA Replication. *Cell* 162, 328–337 (2015). [PubMed: 26165942]
- Locke JCW, Young JW, Fontes M, Jiménez MJH & Elowitz MB Stochastic Pulse Regulation in Bacterial Stress Response. *Science* 334, 366–369 (2011). [PubMed: 21979936]
- Prindle A et al. Ion channels enable electrical communication in bacterial communities. *Nature* 527, 59–63 (2015). [PubMed: 26503040]
- Westers L, Westers H & Quax WJ *Bacillus subtilis* as cell factory for pharmaceutical proteins: a biotechnological approach to optimize the host organism. *Biochim. Biophys. Acta BBA - Mol. Cell Res* 1694, 299–310 (2004).
- van Dijl J & Hecker M *Bacillus subtilis*: from soil bacterium to super-secreting cell factory. *Microb. Cell Factories* 12, 3 (2013).
- Radeck J et al. The *Bacillus* BioBrick Box: generation and evaluation of essential genetic building blocks for standardized work with *Bacillus subtilis*. *J. Biol. Eng* 7, 29 (2013). [PubMed: 24295448]
- Guiziou S et al. A part toolbox to tune genetic expression in *Bacillus subtilis*. *Nucleic Acids Res* 44, 7495–7508 (2016). [PubMed: 27402159]
- Popp PF, Dotzler M, Radeck J, Bartels J & Mascher T The *Bacillus* BioBrick Box 2.0: expanding the genetic toolbox for the standardized work with *Bacillus subtilis*. *Sci. Rep* 7, 15058 (2017). [PubMed: 29118374]
- Wu S-C & Wong S-L Engineering of a *Bacillus subtilis* Strain with Adjustable Levels of Intracellular Biotin for Secretory Production of Functional Streptavidin. *Appl Env. Microbiol* 68, 1102–1108 (2002). [PubMed: 11872456]
- Yansura DG & Henner DJ Use of the *Escherichia coli* lac repressor and operator to control gene expression in *Bacillus subtilis*. *Proc. Natl. Acad. Sci* 81, 439–443 (1984). [PubMed: 6420789]
- Kim L, Mogk A & Schumann W A xylose-inducible *Bacillus subtilis* integration vector and its application. *Gene* 181, 71–76 (1996). [PubMed: 8973310]
- Conrad B, Savchenko RS, Breves R & Hofemeister J A T7 promoter-specific, inducible protein expression system for *Bacillus subtilis*. *Mol. Gen. Genet. MGG* 250, 230–236 (1996). [PubMed: 8628223]
- Bhavsar AP, Zhao X & Brown ED Development and Characterization of a Xylose-Dependent System for Expression of Cloned Genes in *Bacillus subtilis*: Conditional Complementation of a Teichoic Acid Mutant. *Appl Env. Microbiol* 67, 403–410 (2001). [PubMed: 11133472]
- Bongers RS, Veening J-W, Wieringen MV, Kuipers OP & Kleerebezem M Development and Characterization of a Subtilin-Regulated Expression System in *Bacillus subtilis*: Strict Control of Gene Expression by Addition of Subtilin. *Appl Env. Microbiol* 71, 8818–8824 (2005). [PubMed: 16332878]
- Chen PT, Shaw J-F, Chao Y-P, David Ho T-H & Yu S-M Construction of Chromosomally Located T7 Expression System for Production of Heterologous Secreted Proteins in *Bacillus subtilis*. *J. Agric. Food Chem* 58, 5392–5399 (2010). [PubMed: 20377228]
- Toymentseva AA, Schrecke K, Sharipova MR & Mascher T The LIKE system, a novel protein expression toolbox for *Bacillus subtilis* based on the *liaI* promoter. *Microb. Cell Factories* 11, 143 (2012).

17. Dubendorf JW & Studier FW Controlling basal expression in an inducible T7 expression system by blocking the target T7 promoter with lac repressor. *J. Mol. Biol* 219, 45–59 (1991). [PubMed: 1902522]
18. Guzman LM, Belin D, Carson MJ & Beckwith J Tight regulation, modulation, and high-level expression by vectors containing the arabinose PBAD promoter. *J. Bacteriol* 177, 4121–4130 (1995). [PubMed: 7608087]
19. Lutz R & Bujard H Independent and Tight Regulation of Transcriptional Units in *Escherichia Coli* Via the LacR/O, the TetR/O and AraC/I1-I2 Regulatory Elements. *Nucleic Acids Res* 25, 1203–1210 (1997). [PubMed: 9092630]
20. Chen X et al. An extraordinary stringent and sensitive light-switchable gene expression system for bacterial cells. *Cell Res* 26, 854–857 (2016). [PubMed: 27311594]
21. Britton RA et al. Genome-Wide Analysis of the Stationary-Phase Sigma Factor (Sigma-H) Regulon of *Bacillus subtilis*. *J. Bacteriol* 184, 4881–4890 (2002). [PubMed: 12169614]
22. Pédelacq J-D, Cabantous S, Tran T, Terwilliger TC & Waldo GS Engineering and characterization of a superfolder green fluorescent protein. *Nat. Biotechnol* 24, 79–88 (2006). [PubMed: 16369541]
23. Lou C, Stanton B, Chen Y-J, Munsky B & Voigt CA Ribozyme-based insulator parts buffer synthetic circuits from genetic context. *Nat. Biotechnol* 30, 1137–1142 (2012). [PubMed: 23034349]
24. Castillo-Hair SM et al. FlowCal: A User-Friendly, Open Source Software Tool for Automatically Converting Flow Cytometry Data from Arbitrary to Calibrated Units. *ACS Synth. Biol* 5, 774–780 (2016). [PubMed: 27110723]
25. Quisel JD, Burkholder WF & Grossman AD In Vivo Effects of Sporulation Kinases on Mutant Spo0A Proteins in *Bacillus subtilis*. *J. Bacteriol* 183, 6573–6578 (2001). [PubMed: 11673427]
26. van Gestel J, Weissing FJ, Kuipers OP & Kovács ÁT Density of founder cells affects spatial pattern formation and cooperation in *Bacillus subtilis* biofilms. *ISME J* 8, 2069–2079 (2014). [PubMed: 24694715]
27. Studier FW & Moffatt BA Use of bacteriophage T7 RNA polymerase to direct selective high-level expression of cloned genes. *J. Mol. Biol* 189, 113–130 (1986). [PubMed: 3537305]
28. Süel GM, Garcia-Ojalvo J, Liberman LM & Elowitz MB An excitable gene regulatory circuit induces transient cellular differentiation. *Nature* 440, 545–550 (2006). [PubMed: 16554821]
29. Haima P, Bron S & Venema G The effect of restriction on shotgun cloning and plasmid stability in *Bacillus subtilis* Marburg. *Mol. Gen. Genet. MGG* 209, 335–342 (1987). [PubMed: 2823077]
30. Zeigler DR et al. The Origins of 168, W23, and Other *Bacillus subtilis* Legacy Strains. *J. Bacteriol* 190, 6983–6995 (2008). [PubMed: 18723616]
31. Fujita M & Losick R An investigation into the compartmentalization of the sporulation transcription factor  $\sigma^E$  in *Bacillus subtilis*. *Mol. Microbiol* 43, 27–38 (2002). [PubMed: 11849534]
32. Landry BP, Palanki R, Dyulgyarov N, Hartsough LA & Tabor JJ Phosphatase activity tunes two-component system sensor detection threshold. *Nat. Commun* 9, 1433 (2018). [PubMed: 29650958]
33. Engler C, Gruetzner R, Kandzia R & Marillonnet S Golden Gate Shuffling: A One-Pot DNA Shuffling Method Based on Type IIs Restriction Enzymes. *PLoS ONE* 4, e5553 (2009). [PubMed: 19436741]
34. Zadeh JN et al. NUPACK: Analysis and design of nucleic acid systems. *J. Comput. Chem* 32, 170–173 (2011). [PubMed: 20645303]
35. Eswaramoorthy P, Guo T & Fujita M In Vivo Domain-Based Functional Analysis of the Major Sporulation Sensor Kinase, KinA, in *Bacillus subtilis*. *J. Bacteriol* 191, 5358–5368 (2009). [PubMed: 19561131]
36. Fujita M Temporal and selective association of multiple sigma factors with RNA polymerase during sporulation in *Bacillus subtilis*. *Genes Cells Devoted Mol. Cell. Mech* 5, 79–88 (2000).
37. Harwood CR & Cutting SM *Molecular biological methods for Bacillus* (Wiley, 1990).
38. Newville M et al. Lmfit: Non-Linear Least-Square Minimization and Curve-Fitting for Python. *Astrophys. Source Code Libr* (2016).

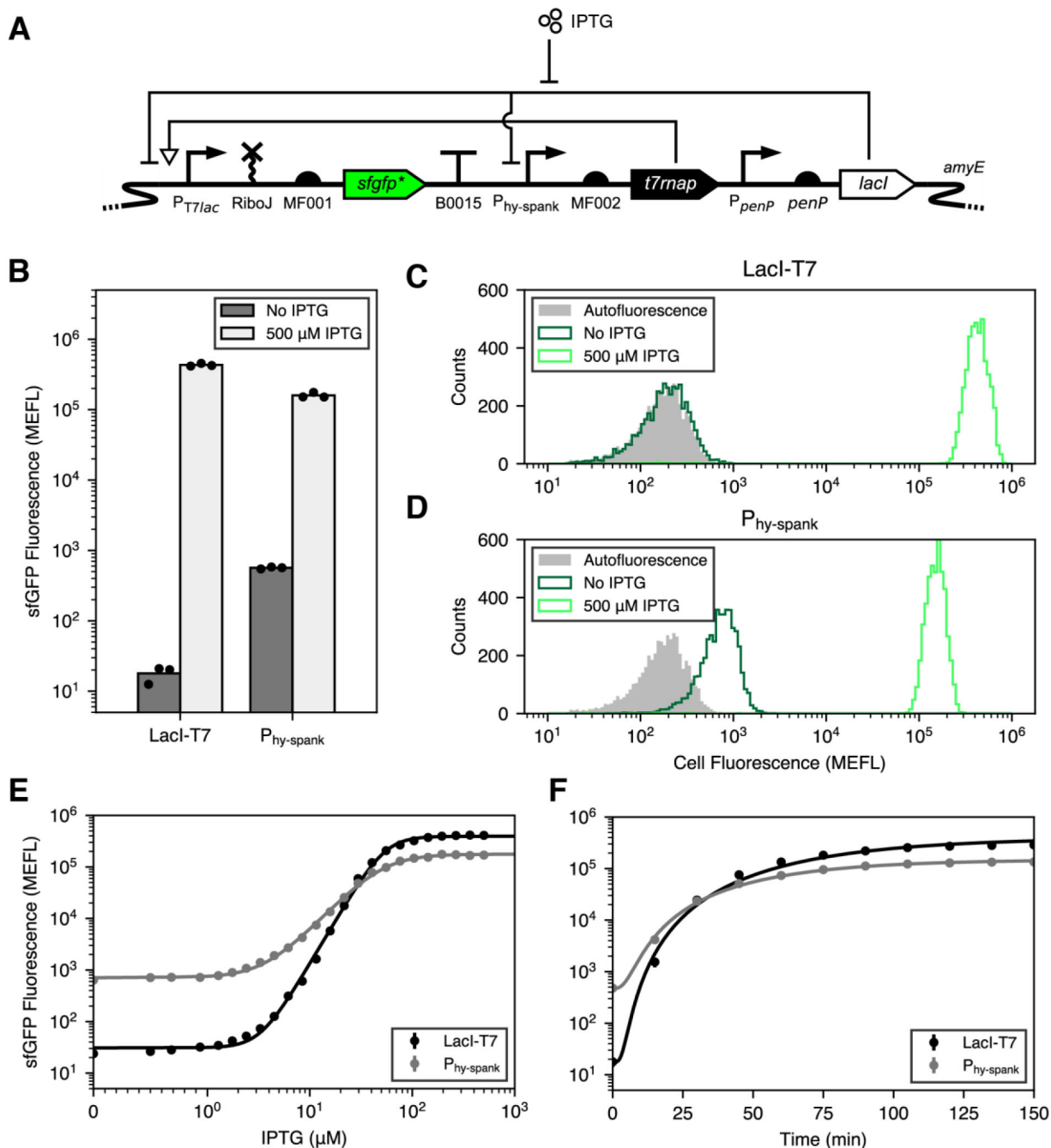


**Figure 1. LacI-T7 design and performance.**

(A) Genetic device schematic of LacI-T7 with regulatory interactions shown. (B) sfGFP fluorescence from LacI-T7 and  $P_{hy-spank}$  in the absence or presence of IPTG. Fluorescence is shown in calibrated Molecules of Equivalent Fluorescein (MEFL) units. Bars represent the mean of three experimental replicates run on separate days. Dots show the values of the individual replicates. (Methods). (C and D) Representative flow cytometry histograms of autofluorescence control (*B. subtilis* lacking any *sfgfp* gene), and those with *sfgfp* under either LacI-T7 (C) or  $P_{hy-spank}$  (D), in the presence or absence of IPTG. (E) sfGFP

Fluorescence from LacI-T7 and  $P_{hy\text{-spank}}$  as a function of IPTG concentration. **(F)** sfGFP fluorescence from LacI-T7 and  $P_{hy\text{-spank}}$  after addition of saturating IPTG. Dots and error bars show the mean and standard deviation, respectively, of three experiments run on separate days. Error bars are, in most cases, smaller than the size of the dots, and thus not visible. Black lines represent model fits (Methods).

Author Manuscript

Author Manuscript

Author Manuscript

Author Manuscript